Australian Journal of Basic and Applied Sciences, 5(3): 120-133, 2011
ISSN 1991-8178

Electromagnetic (EM) Absorption Rate Reduction of Helix Antenna with Shielding Material for Mobile Phone Application

[1]Mohammad Tariqul Islam, [1,2]Mohammad Rashed Iqbal Faruque, [1,2]Norbahiah Misran

[1]Institute of Space Science (ANGKASA),
[2]Dept. of Electrical, Electronic and Systems Engineering, Faculty of Engineering and Built Environment, Universiti Kebangsaan Malaysia, 43600 UKM, Bangi, Selangor, Malaysia.

Abstract: This paper proposes the reduction of specific absorption rate (SAR) with shielding material is performed by the finite-difference time-domain method (FDTD) with lossy-Drude model by CST Microwave Studio. We propose SAR evaluation and reduction methods based on power conservation. It has been shown that even though the use of shielding (ferrite) material not only reduces the SAR in the human head but also the radiated power, it reduces the SAR in head more considerably than the radiated power. Shielding materials have achieved a 58.68% reduction of the initial SAR value for the case of 1 gm SAR. These results suggest a guideline to choose various types of materials with the maximum SAR reducing effect for a phone model.

Key words: antenna, human head model, FDTD method, Shielding materials, SAR.

INTRODUCTION

The portable terminal devices are commonly used in the human life. As usages of the mobile devices are increased, the study about the health risk from the exposure electromagnetic fields is widely in movement. The basic safety limits for radio frequency exposure are defined in terms of absorbed power per unit mass, which is expressed by SAR in W/Kg [Byun and Lee, 2001; Islam *et al*., 2009]. Depending on the exposure condition, SAR is expressed either as a localized SAR value or averaged over the whole body. It describes the amount of energy W absorbed in a dielectric material in time (d*t*) and mass unit (d*m*).

$$SAR = \frac{d}{dt}\left(\frac{dW}{dm}\right) \tag{1}$$

It can be related to the electric field or temperature rise (d*T*) at a point by

$$SAR = \frac{\sigma_{eff}\left|E\right|_{rms}^{2}}{\rho} = \left(\sigma + \omega\varepsilon_0\varepsilon''\right)\frac{\left|E\right|^{2}}{\rho} = c\frac{dT}{dt}. \tag{2}$$

Where E is the root-mean-square (rms) electric field; σ_{eff} is the effective conductivity (S/m); ρ is the mass density (kg/m^3); $\omega = 2\pi f$, with f the frequency; ε_0 is the permittivity of free space; ε^{11} is the loss factor and c is the specific heat capacity (J/kg/^{0}C) of the material.

In case of cellular phone services such as mobile or PCS (Personal Communication Services), the SAR value must not excess the exposure guidelines [ICNIRP Guidelines, 1988]. Therefore, it is important issue of the cellular phone devices that reduction of electromagnetic (EM) absorption radiation. Previously, electromagnetic band gap (EBG) attached with antenna and human head, a position study of the antenna feeding point and a use of the metamaterial with split ring resonator structure were proposed to reduction of SAR value [Kwak ., 2009; Islam ., 2010].

Recently, there are many interests on ferrite material to design high performance devices such as low profile structure, to enhance antenna gain and to reduce of SAR value [Islam ., 2009], [Wang and Fujiara, 1999]. The ferrite material has high electromagnetic surface impedance, which is capable of suppressing current and act as perfect electromagnetic conductor in certain frequency range. Also ferrite material can reduce the

Corresponding Author: Mohammad Tariqul Islam, Institute of Space Science (ANGKASA),

surface waves which are generated EM wave towards the human head.

The interaction of handset antennas with the human body is a great consideration in cellular communications. The user's body, especially the head and hand, influence the antenna voltage standing wave ratio (VSWR), gain, and radiation patterns. Furthermore, thermal effects, when tissues are exposed to unlimited electromagnetic energy, can be a serious health hazard [Islam ., 2009; ICNIRP Guidelines, 1988; Kwak ., 2009].

Some gain degradation is usually observed when a handset is held by hand and operated in the surrounding area of a human head at the talk position [Ishimaru, 1991; Magdy, 2000; Li ., 1997]. This is mainly caused by variation of currents flowing on the conducting materials such as a shielding box or a ground plane in the handset unit. The currents on these materials are induced by the excitation of the antenna element and contribute to radiation as well as to the antenna element. Thus the handset body is treated as a part of the radiator when designing handset antenna systems. It has been shown that the distribution of these currents varies depending on the type, position and feed point of the antenna element, and also on the dimensions of the antenna element and the handset unit [Ishimaru, 1991], [Cabedo ., 2009; Morishita ., 2002; Chi ., 2008; Boyle ., 2007; Arenas ., 2009]

In this paper the authors suggest on the effects of attaching positions of the shielding materials to cellular phone for SAR reduction has been presented. It is shown that the position of the shielding material is an important factor for SAR reduction effectiveness. There is a necessity to make an effort for reducing the spatial peak SAR in the design stage of the shielding material because the possibility of a spatial peak SAR exceeding the recommended exposure limit cannot be completely ruled out. Even though, we propose also SAR assessment and reduction methods based on power conservation relation. The authors analyze the SAR data as a function of shielding material length monitoring the current distribution on the conducting box of the handset. We also compare the SAR in case of using flip type handset with that in case of a folder type handset.

MATERIALS AND METHOD

The simulation model which includes the handset with helix type of antenna and the SAM phantom head provided by CST Microwave Studio (CST MWS) is shown in Fig. 1. Complete handset model composed of the circuit board, LCD display, keypad, battery and housing was used for simulation. The relative permittivity and conductivity of individual components were set to comply with industrial standards.

Fig. 1: Complete model used for simulation including handset and SAM phantom head

In addition, definitions in [Islam , 2009; Wang and Fujiara, 1999] were adopted for material parameters involved in the SAM phantom head. In order to accurately characterize the performance over broad frequency range, dispersive models for all the dielectrics were adopted during the simulation [Islam ., 2009].

Table 1: Electrical properties of materials used for simulation

Phone Materials	ε_r	σ (S/m)
Circuit Board	4.4	0.05
Housing Plastic	2.5	0.005
LCD Display	3.0	0.02
Rubber	2.5	0.005
SAM Phantom Head		
Shell	3.7	0.0016
Liquid @ 900 MHz	40	1.42

The electrical properties of materials used for simulation are listed in Table 1. Helix type antenna constructed in a helical sense operating at 900MHz for GSM application was used in the simulation model. In order to obtain high-quality geometry approximation for such helical structure, predictable meshing scheme used in FDTD method usually requires large number of hexahedrons which in turn makes it extremely challenging to get convergent results within reasonable simulation time.

A total of 2,097,152 mesh cells were generated for the complete model, and the simulation time was 1163 seconds (including mesh generation) for each run on an Intel Core TM 2 Duo E 8400 3.0 GHz CPU with 4GB RAM system.

III. Analysis of SAR Reduction Method:

III. A. Power Conservation:

Power conservation is considered to be one of the choices we can take to reduce SAR caused by a handset. This technique is followed by FDTD method. Fig. 2 shows the power conservation in which the antenna input power P_{in} consists of the absorbed power in the head (P_h), (volume V_h), the absorbed power in ferrite material (P_f) if used (volume V_f), and the radiated power (P_r) flowing out of the surface S.

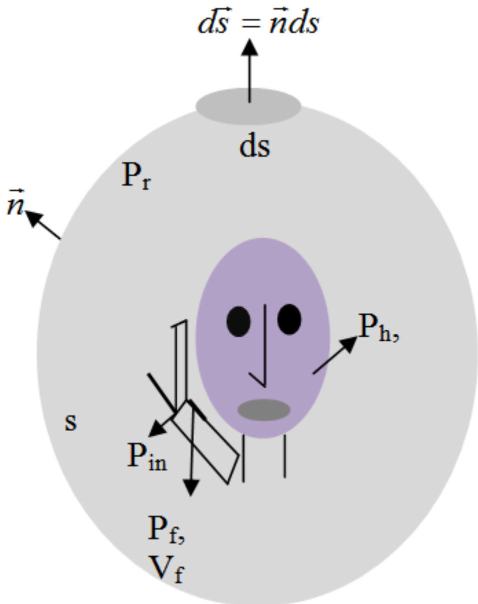

Fig. 2: Power conservation

$$P_{in} = \frac{1}{2}\mathrm{Re}\left(VI^*\right) = P_h + P_f + P_r$$

$$= \frac{1}{2}\int_{V_h} \sigma_1 \left|\vec{E}\right|^2 dv + \frac{1}{2}\int_{V_f}\left(\sigma_1\left|\vec{E}\right|^2 + \sigma_2\left|\vec{H}\right|^2\right)dv \tag{3}$$

$$+\frac{1}{2}\mathrm{Re}\left[\int_{s}\left(\vec{E}\times\vec{H}^*\right).\vec{ds}\right].$$

where V, I, $\vec{E}$, and $\vec{H}$ are antenna input voltage, antenna input current, electric field, and magnetic field expressed in passers. The symbols σ_1, σ_2, and * are electric conductivity, magnetic conductivity, and complex conjugate. Based on the expression (1), the absorption rate in head, absorption rate in ferrite material, and radiation rate are defined as follows:

Radiation rate $P_r(\%) = \frac{P_r}{P_{in}} \times 100(\%)$. (4)

Absorption rate in head $P_h(\%) = \frac{P_h}{P_{in}} \times 100(\%)$. (5)

Absorption rate in shielding material $P_f(\%) = \frac{P_f}{P_{in}} \times 100(\%)$. (6)

The sum of radiation rate, absorption rate in head, and absorption rate in ferrite material must be always 100(%).

III. B. Evaluation of SAR When Using Shielding Material:

Shielding material is considered to be one of the choices we can take to reduce SAR caused by a handset. The FDTD formulations were derived from the following Maxwell's equation [2]:

$$\frac{\delta \vec{H}}{\delta t} = -\frac{1}{\mu_0 \mu_r'}\left(\nabla \times \vec{E}\right) - \frac{\sigma_2}{\mu_0 \mu_r'}\vec{H}. \quad (7)$$

$$\frac{\delta \vec{E}}{\delta t} = \frac{1}{\varepsilon_0 \varepsilon_r'}\left(\nabla \times \vec{H}\right) - \frac{\sigma_1}{\varepsilon_0 \varepsilon_r'}\vec{E}. \quad (8)$$

where $\vec{E}$ = electric field (V/m), $\vec{H}$ = magnetic field (A/m), ε_0 = permittivity of free space, μ_0 = permeability of free space, ε_r ' =real part of relative permittivity, $\mu_r^{'}$= real part of relative permeability, electric conductivity $\sigma_1 = \omega \varepsilon_0 \varepsilon_r^{''}$ (Ω/m), and magnetic conductivity $\sigma_2 = \omega \mu_0 \mu_r^{''}$ (Ω/m), respectively. To see the effects of SAR reduction in the human head, the shielding material that has electric and magnetic losses ($\varepsilon_{r = 7\text{-}j\,0.6}$, $\mu_{r= 2.8\text{-}j3.3}$) is used in simulations. Since the ferrite material generally absorbs EM energy, if it is attached on handsets, it is natural that it reduces some SAR value in head. However, since this also reduces the radiated power in most cases, we need to be somewhat careful to handle this problem. To evaluate the effects of SAR reduction in a more quantitative manner, we defined SRF (SAR Reduction Factor) as follows:

$$SRF_{Total}(\%) = \frac{P_h - P_{h,f}}{P_h} \times 100. \quad (7)$$

$$SRF_{1gm}(\%) = \frac{SAR_{1gm} - SAR_{1gm,f}}{SAR_{1gm}} \times 100. \quad (8)$$

$$SRF_{10gm}(\%) = \frac{SAR_{10gm} - SAR_{10gm,f}}{SAR_{10gm}} \times 100. \quad (9)$$

where SRF_{Total} is SRF for absorbed power in entire head, SRF_{1gm} is SRF for 1gm peak SAR, SRF_{10gm} is SRF for 10gm peak SAR, P_h is absorbed power in head assuming that ferrite material is not used, P_{hf} , is absorbed power in head assuming that ferrite material is used, SAR_{1gm} is 1gm peak SAR (without ferrite), $SAR\ 1_{gm\,f}$, is 1gm peak SAR (ferrite), SAR_{10gm} is 10gm peak SAR (without ferrite), and $SAR\ 10_{gm\,f}$, is 10gm peak SAR (ferrite), respectively. The values of $P_{h\,f}$, $SAR\ _{1gm\,f}$, and $SAR\ 10gm\ f$, are properly scaled based on the same radiated power as in the case of without ferrite material. It should be noted that, the lager the calculated SRF value is, the greater the SAR reduction effect.

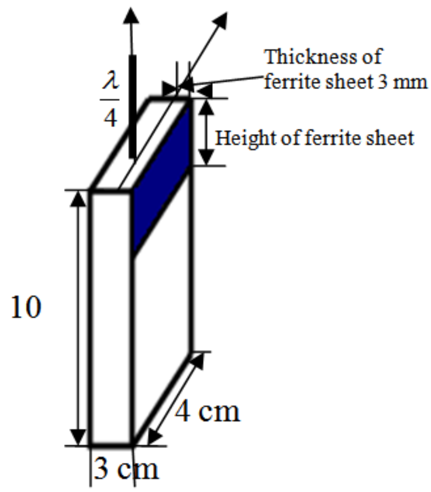

(a) Geometry of handset antenna

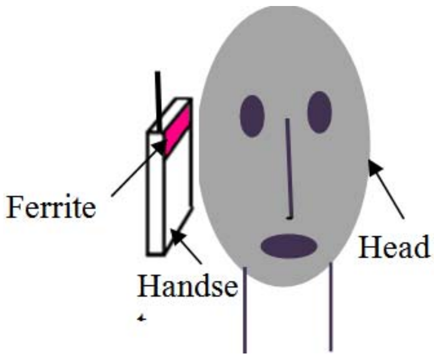

(b) Head Model

Fig. 3: Geometry for handset with ferrite sheet and head model

Fig. 3 shows the geometry for the handset with ferrite material and human head. The mobile handset is assumed to be located 10 mm away from the edge of the ear. The angle between the mobile handset and the upright head is 30° and the thickness of the ferrite material is 3 mm. In the simulations, the authors used CST Microwave Studio, which includes biological database of human head. The head database consists of seven biological tissues (cartilage, muscle, eye, brain, skin, bone, and blood). Table-2 and Table-3 show that dielectric tissue property for 900 MHz and 1800 MHz [Chiu ., 2009; Kouveliotis ., 2006; Sievenpiper, 1999]. A quarter-wavelength helix antenna (center frequency=1.81GHz) is assumed to be mounted on a rectangular metal box.

Table 2: Dielectric tissue properties at 900 MHz

Materials	Density, ρ (kg/m^3)	Conductivity, σ (S/m)	Relative permittivity ε_r
Cartilage, Bone	1130	0.12	4.83
Muscle, Skin	1020	1.50	50.50
Brain	1050	1.11	41.70
Eye	1000	2.03	68.60
Blood	1060	1.54	61.36

Table 3: Dielectric tissue properties at 1800 MHz

Materials	Density, ρ (kg/m^3)	Conductivity, σ (S/m)	Relative permittivity ε_r
Cartilage, Bone	1130	0.11	4.48
Muscle, Skin	1020	1.35	47.80
Brain	1050	1.09	39.50
Eye	1000	1.99	65.30
Blood	1060	1.51	58.35

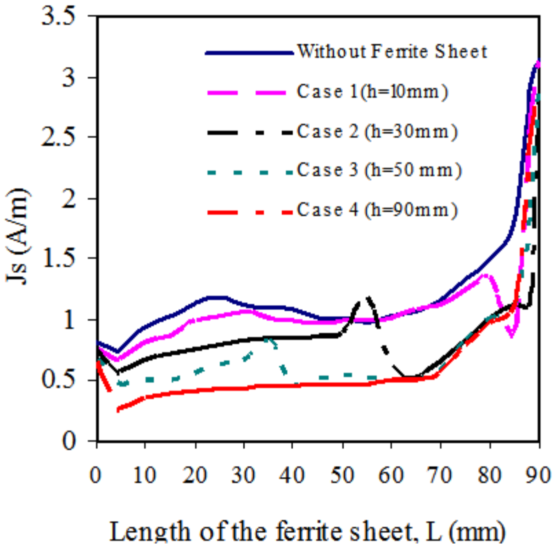

Fig. 4: Current distributions with compared ferrite length.

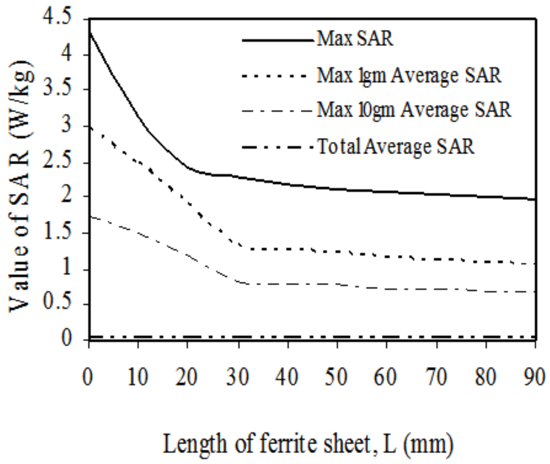

Fig. 5: SAR value with compared as a ferrite length

Fig. 4 shows the surface current distribution on the conducting plane as a function of ferrite length (3~9 mm) assuming the input power of 600 mW. When the ferrite length is longest (90 mm), the surface current density is reduced approximately 51% that's why ferrite length is the important factor for surface current distribution.

In Fig. 5 shows the various SAR values assuming the same conditions as in Fig, 4. From this Fig. 5 shows that SAR value is reduced about 48.68% when the ferrite material length is 30 mm and they are saturated. The results implies that only suppressing the maximum current on the front side of the conducting box contributes significantly to the reduction of spatial peak SAR. This is because the decreased quantity of the power absorbed in the head is considerably larger than that dissipated in the ferrite material. To verify the SAR reduction effect in terms of the SRF (SAR Reduction Factor) defined earlier, The SRF values are computed as a function of fer rite length and are summarized in Table 4. For example, the SRF_{total} is calculated as $\left(P_h - P_{h,f} \times P_r / P_{r,f}\right) / P_h$, where P_r is radiated power without the ferrite material and $P_{r,f}$, is the radiated power with the ferrite material. We can see that the SRF increases as the length of the ferrite material increases but is saturated beyond 30 mm.

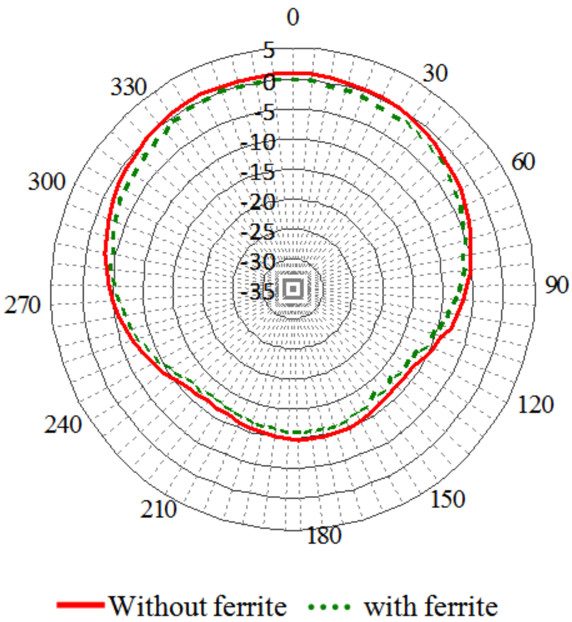

Fig. 6(a): Radiation pattern (Φ =0°) with and without ferrite material

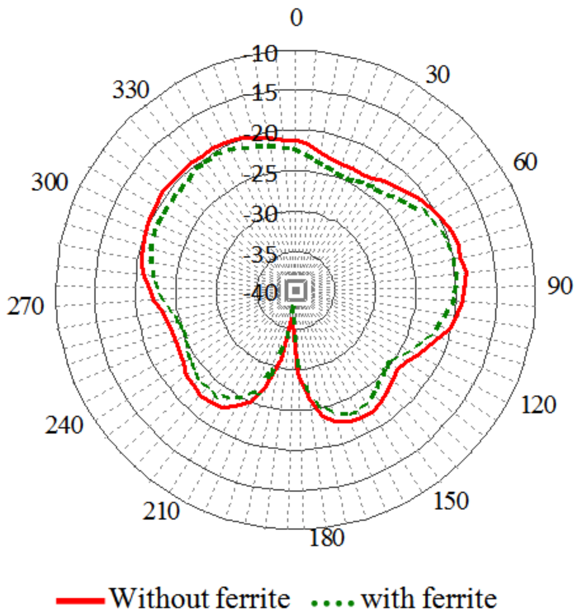

Fig. 6(b): Radiation pattern (Φ =0°) with and without ferrite material

From this Fig. 6 shows the radiation pattern with and without ferrite material in the plane of Φ =0°. Also, Fig. 6 shows that these radiation patterns, the authors examine that with ferrite, the cross-polarization field decreases more considerably than the co-polarization field.

Also, Fig. 7 shows the return losses of the antenna as a function of the ferrite length. It is shown that they do not change much as the ferrite length is varied.

The different size of ferrite material was chosen as a candidate for reducing the EM absorption in the human head. Fig. 8 shows the three sizes of the ferrite material, named Category 1, Category 2, and Category 3 were considered in this study. Category 1 showed the case where a phone model is inserted in a thin dielectric case including a ferrite material 4 × 3 cm in the area above the antenna feed point. Category 2 showed the case for a ferrite sheet of 4 × 3 cm covering one part of the phone model below the antenna feed point. Category 3 had a size twice as large as Category 1, and Category 2.

Table 4: Ferrite lengths with compared SRF

Length of ferrite material	$SRF_{Total (\%)}$	$SRF_{1 gm}$ (%)	$SRF_{10 gm}$(%)
10 mm	9.32	-0.21	3.11
20 mm	19.2	20.84	23.96
30 mm	26.98	46.37	46.16
40 mm	32.33	47.76	45.37
50 mm	35.98	47.99	45.14
60 mm	36.11	47.88	45.27
70 mm	36.73	47.79	45.89
80 mm	36.98	47.68	46.33
90 mm	37.2	47.61	47.11

Table 5: Effects of the attaching locations of ferrite sheet on SAR reduction at 900 MHz

	ξ[%]		
	1800 MHz		
Peak SAR 1 gm for head	46.87	47.68	58.68
Peak SAR 1 gm for brain	46.59	47.77	58.92
Average SAR for eye ball	4.9	12.34	12.94
Average SAR for head	32.13	32.01	39.57
P_{abs} by head	32.13	32.01	39.57

Table 6: Effects of the attaching locations of ferrite sheet on SAR reduction at 1800 MHz

	ξ[%]		
	1800 MHz		
	Category 1	Category 2	Category 3
Peak SAR 1 gm for head	48.98	48.69	61.32
Peak SAR 1 gm for brain	46.60	51.53	63.50
Average SAR for eye ball	11.23	31.74	37.74
Average SAR for head	34.54	37.57	43.21
P_{abs} by head	34.54	37.57	43.21

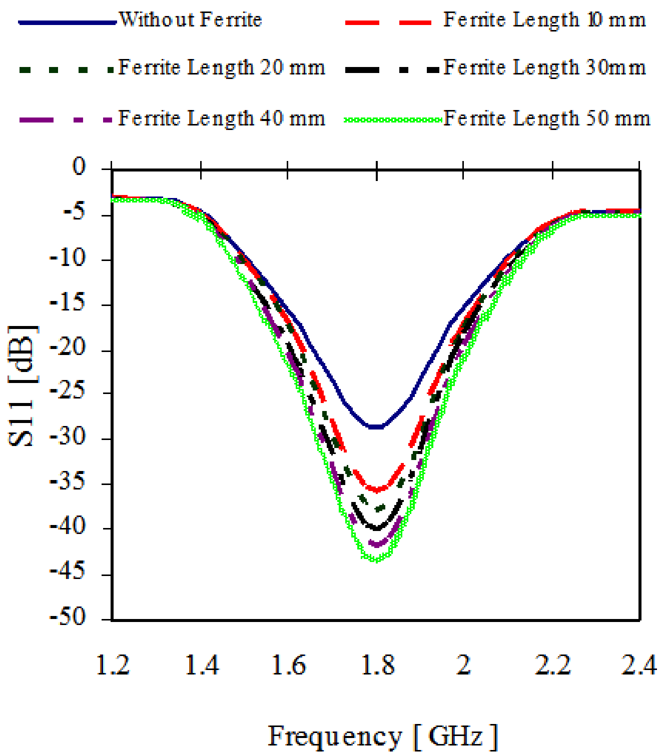

Fig. 7: Return losses as a purpose of ferrite length

Table-5 and Table-6 depicted that the ξ calculated for the three types of ferrite sheet. It can be seen that all of the ferrite sheets gives a significant reduction of EM absorption at both 900 MHz and 1800 MHz. A reduction of 47- 49 % on the peak SAR 1 gm can be obtained from Category 1, and Category 2, and a reduction over 58.68 % on the peak SAR 1 gm can be obtained from Category 3. A double sheet size has not

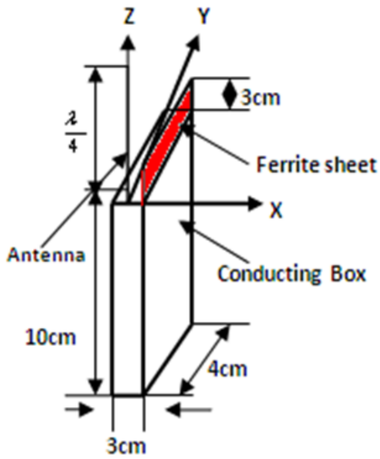

(A)

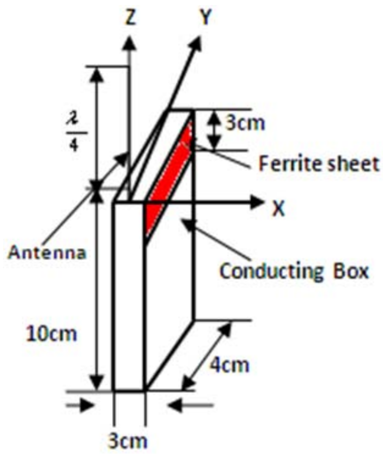

(B)

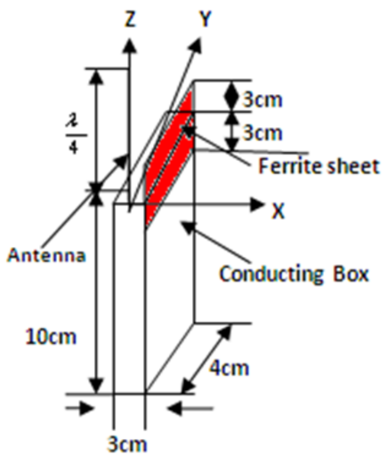

(C)

Fig. 8: Phone model with ferrite sheets. (A) Category 1 (B) Category 2 (C) Category 3

given a double reduction effect because the current on the monopole degrades with deviating from the antenna feed point. The numerical results for Category 1 and Category 2 also show that the ferrite materials above and below the feed point have the same effect on the reduction of EM absorption provided they have the same size. This fact suggests that Category 2 is more realistic from a view point of practical use. So in the following the numerical results and discussions are limited to Category 2. Since the ferrite material is an EM absorptive one, the attaching positions and size of ferrite sheet may be an important factor for the reduction of EM absorption.

III. C. Absorbing Characteristics in Case of Plane Incidence Wave:

In order to estimate the permittivity and permeability of a layer to absorb maximum power, we first consider the case of N dielectric layers as shown in fig. 9. The thickness and complex relative permittivity of the m-th layer is given by d_m and ε_m respectively. The reflection and transmission coefficients are given by [Wang anfd Fujiara, 1999]:

$$R = \frac{A + B/Z_i - Z_i(C + D/Z_i)}{A + B/Z_i + Z_i(C + D/Z_i)}, \tag{12a}$$

$$T = \frac{2}{A + B/Z_i + Z_i(C + D/Z_i)} \tag{12b}$$

In equation 12(a) and 12(b), A, B, C, and D are elements of the ABCD matrix given by

$$\begin{bmatrix} A & B \\ C & D \end{bmatrix} = \begin{bmatrix} A_1 & B_1 \\ C_1 & D_1 \end{bmatrix} \cdots \begin{bmatrix} A_m & B_m \\ C_m & D_m \end{bmatrix} \cdots \begin{bmatrix} A_n & B_n \\ C_n & D_n \end{bmatrix} \tag{13}$$

Where $A_m = D_m = \cos(\beta_m d_m)$, $B_m = jZ_m \sin(\beta_m d_m)$, $C_m = j\sin(\beta_m d_m)/Z_m$, $\beta_m = k_m \cos(\theta_m)$, and $k_m = k_0 \sqrt{n_m}$. The symbols ω is the radiation frequency, c is the velocity of light, k_0 is the free space wave numbering the m-th layer, and β_m is the propagation constant in Z direction. For the perpendicularly and parallel polarized incident fields, the wave impedance Z_m's, which are defined as the ratio of the transverse electric and magnetic fields, result in

$$Z_m = \eta_m / \cos\theta_m \tag{14}$$

and

$$Zm = \eta_m \cos\theta_m \tag{15}$$

respectively, where η_m is the intrinsic impedance of the m-th layer given by

$$\eta_m = \sqrt{\frac{\mu_m}{\varepsilon_m}} = \sqrt{\frac{\mu_0 \mu_m}{\varepsilon_0 \varepsilon_m}} = \frac{120\pi}{\sqrt{\varepsilon_m}} \tag{16}$$

$\mu_m = 1$ is assumed.

Because the absorbing material attached on handsets is usually single-layered, we assume that N =1. To estimate the permittivity and permeability, which enable maximum absorbed power in shielding material, the recursive method can proceed as follows:

Set up the frequency (f), thickness of the ferrite material (t), and the incident angle (θ_i)
Start with the initial permeability value (μ_r =1 or arbitrary value

Determine the permittivity ($\varepsilon_{r1} = \varepsilon'_{r1} - j\varepsilon''_{r1}$) which has maximum absorption in the layer.

Determine the permeability ($\mu_{r1} = \mu'_{r1} - j\mu''_{r1}$) which has maximum absorption in the layer based on the above determined permittivity ($\varepsilon_{r1} = \varepsilon'_{r1} - j\varepsilon''_{r1}$)
Repeated the process
When the absorption rate converges, stop the process
Estimate the permittivity and permeability (ε_{rm}, μ_{rm}).

Fig. 9 shows the permittivity permeability values of a layer with which the maximum power is absorbed for various incident angels (0, 30, 60^0) in case of a perpendicularly polarized incident wave. The permittivity and permeability values, which enable maximum absorption in layer when incident angles are 0, 30, 600, are used as layer characteristics for the cases in category 1, category 2, and category 3 respectively.

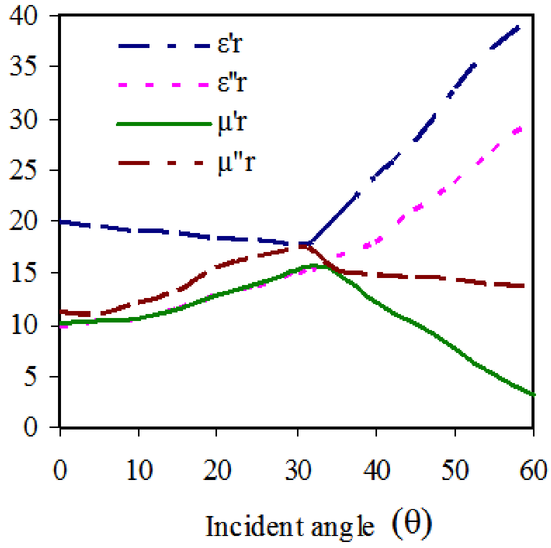

Fig. 9: Permittivity and permeability for maximum absorption

III. D. Study of SAR in Folder Type Handset:

In order to approximate the condition which is close to the typical position of handset over a human head, the position of the folder type handset as shown in Fig. 10, which has a tilt of 60° toward the y direction, and 30° toward the -x direction, is assumed.

In Fig.11, we compute the SAR, P_r (%), and P_h (%) as a function of folder length (L) assuming that the distance between the handset and the edge of the ear is 20 mm. The antenna input power is 600mW, and the center frequency is 1.83GHz. It is shown that the SAR value when using the folder type (L=50 mm) is about 29 % smaller than that when using the flip type (L=0 mm).

Fig. 12 shows the SAR data and the various absorbing ratios as a function of the folder length assuming the same conditions as given for Fig. 11 except that a ferrite material of length 30 mm is attached on the handset. As shown in these data, we can examine that as the length of the folder increases, the absorption rate in ferrite decreases and radiation rate increases. Thus, the SAR-reducing property of the ferrite material when using a flip type handset is not shown to be conspicuous for a folder type one.

IV. Conclusion:

In this paper, we propose SAR evaluation and reduction methods based on power conservation. After defining SRF (SAR Reduction Factor) for a more quantitative discussion of effective SAR reduction methods, many kinds of simulation have been performed. From many parametric studies, it has been shown that even though the use of ferrite material not only reduces the SAR in the head but also the radiated power, it reduces

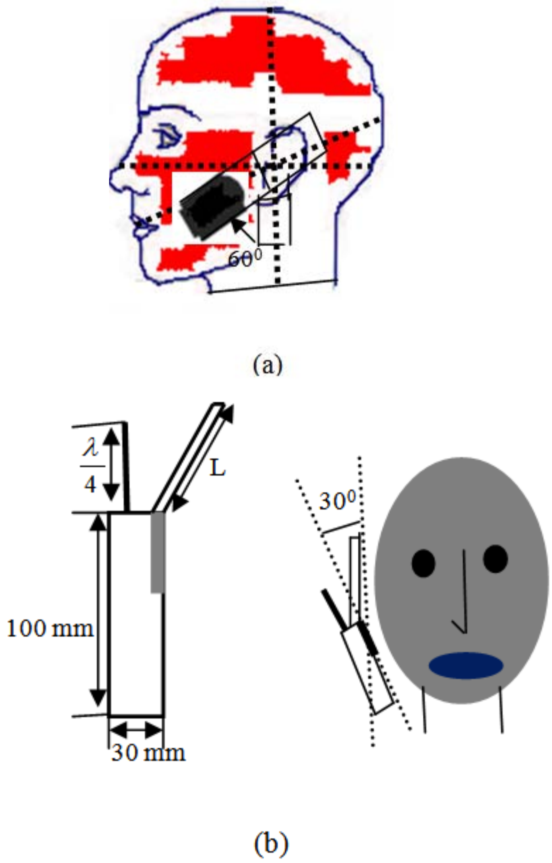

Fig. 10: Position of folder type handset relative to head model.

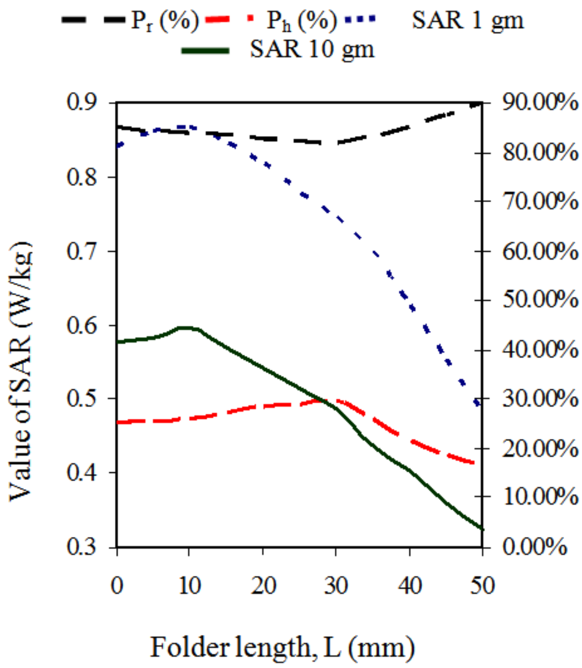

Fig. 11: Folder length with compared SAR value, radiation power and absorption power without ferrite material.

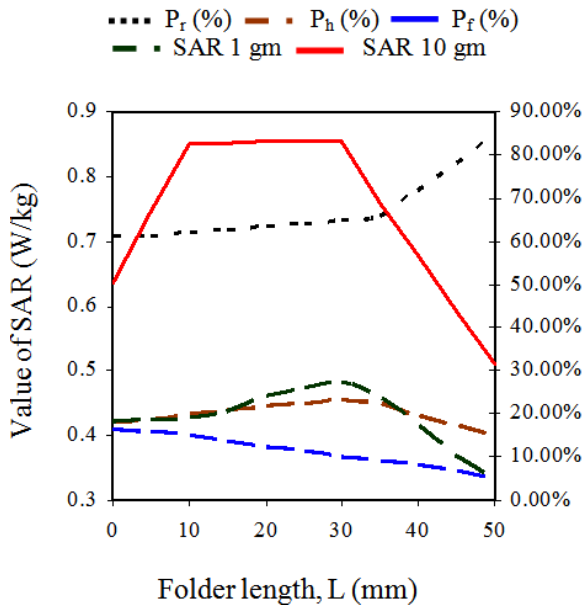

Fig. 12: Folder length with compared SAR value, radiation power and absorption power with ferrite material.

the SAR in head more considerably than the radiated power. Thus the ferrite material may be used in this sense as one of the SAR reduction methods. Ferrite materials have achieved a 55.68% reduction of the initial SAR value for the cases of 1 gm SAR which is the dependent on position on shielding material. We have also shown that in a typical position of handsets over a human head, the SAR when using a folder type is about 29% smaller than that when using a flip type. Numerical results can provide useful information in designing safety cellular phone communication equipment compliance.

ACKNOWLEDGMENT

The authors would like to thank Institute of Space Science (ANGKASA), Universiti Kebangsaan Malaysia (UKM) and the MOSTI Secretariat, Ministry of Science, Technology and Innovation of Malaysia, e- Science fund: 01-01-02-SF0612, for sponsoring this work.

REFERENCES

Arenas, J.J., J. Anguera and C. Puente, 2009. Balanced and single-ended handset antennas: Free space and human loading comparison, Microwave Optical Technology Letters, 51(9): 2248-2254.

Boyle, K.R., Y. Yuan and L.P. Lighthart, 2007. Analysis of mobile phone antenna impedance variations with user proximity, IEEE Transactions on Antennas and Propagation, 55(2): 364-372.

Byun, J., J.H. Lee, 2001. FDTD calculation of SAR for the monopole antenna on the conducting box in terms of the structure nearby feed, IEEE APS, 2: 76-79.

Cabedo, A., J. Anguera, C. Picher, M. Ribo and C. Puente, 2009. Multi-band handset antenna combining PIFA, slots, and ground plane modes, IEEE Transactions on Antennas and Propagation, 57(9): 2526-2533.

Chi, Y.W. and K.L. Wong, 2008. Compact multiband folded loop chip antenna for small-size mobile phone, IEEE Transactions on Antennas and Propagation, 56(12): 3797-3803.

Chiu, C.W. and Y.J. Chi, 2009. Planar hexa-band inverted-F antenna for mobile device applications, IEEE Antenna and Wireless Propagation Letters, 8: 1099-1102.

International Non-Ionizing Radiation Committee of the International Radiation Protection Association, 1988. Guidelines on limits of exposure to radio frequency electromagnetic fields in the frequency range from 100 kHz to 300 GHz, Health Phys., 54(1): 115-123.

Islam, M.T., M.R.I. Faruque and N. Misran, 2009. Design analysis of ferrite sheet attachment for SAR reduction in human head, Progress In Electromagnetics Research, PIER, 98: 191-205.

Islam, M.T., M.R.I. Faruque and N. Misran, 2010. Study of specific absorption rate (SAR) in the human head by metamaterial attachment, IEICE Electronics Express, 7(4): 240-246.

Ishimaru, A., 1991. Electromagnetic Wave Propagation, Radiation, and Scattering, Prentice Hall, pp: 16-17.

Iskander, M.F., 2000. Polarization and human body effects on the microwave absorption in a human head exposed to radiation from handheld devices, IEEE Trans. Microwave Theory and Techniques, 48(11): 1979-1987.

Kwak. S.I., D.U. Sim, J.H. Kwon and H.D. Choi, 2009. Experimental tests of SAR reduction on mobile using EBG structures, Electron. Lett., 44(9): 568-570.

Kouveliotis, K., S.C. Panagiotou, P.K. Varlamos and C.N. Capsalis, 2006. Theoretical approach of the interaction between a human head model and a mobile handset helical antenna using numerical methods, Progress In Electromagnetics Research, PIER, 65: 309-327.

Le, W. Li, Pang S. Kooi, Mook S. Leign, Hse M. Chan, Tat S. Yeo, 1997. FDTD analysis of electromagnetic interactions between handset antennas and the human head, *AP Microwave conf*., pp: 1189-1192.

Morishita, H., H. Furuuchi and K. Fujimoto, 2002. Performance of balanced-fed antenna system for handsets in the vicinity of a human head or hand, IEE Proceedings on Microwave, Antennas and Propagation, 149(2): 85-91.

Sievenpiper, D., 1999. High-impedance electromagnetic surfaces with a forbidden frequency band, IEEE Trans. Microw. Theory Tech., 47: 2059-2074.

Wang, J. and O. Fujiwara, 1999. FDTD computation of temperature rise in the human head for portable telephones, IEEE Trans. Microwave Theory Tech., 47(8): 1528-1534.